R. & M. No. 3147
(20,471)
A.R.C. Technical Report

R. & M. No. 3147

MINISTRY OF AVIATION

AERONAUTICAL RESEARCH COUNCIL
REPORTS AND MEMORANDA

A Note on the Theory of the Stanton Tube

By G. E. GADD, Ph.D.
OF THE AERODYNAMICS DIVISION, N.P.L.

LONDON: HER MAJESTY'S STATIONERY OFFICE
1960
FOUR SHILLINGS NET

A Note on the Theory of the Stanton Tube

By G. E. GADD, Ph.D.

OF THE AERODYNAMICS DIVISION, N.P.L.

*Reports and Memoranda No. 3147**

October, 1958

Summary.—Existing theories for the Stanton tube are critically reviewed, and the paper then outlines a simple method which predicts the calibration function at high Reynolds numbers to the right order of magnitude.

The Stanton tube, first used by Stanton, Marshall, and Bryant[1] to investigate the laminar sublayer of a turbulent flow, has the general form shown in Fig. 1. Its width is usually very much greater than its height d, so that the flow over it is effectively two-dimensional. The instrument may be calibrated by, for example, placing it in a duct whose walls are far apart compared with the tube height. The skin friction τ_w can be deduced from the pressure drop along the duct. If the Stanton tube reads a pressure Δp higher than the local static pressure, a suitable non-dimensional way of presenting the calibration results is, following Taylor[2] with some modifications, to plot the ratio d'/d against R_s, where

$$d' \equiv \left(2\frac{\Delta p}{\rho}\right)^{1/2}\frac{\mu}{\tau_w}, \tag{1}$$

$$R_s \equiv \frac{\rho}{\mu^2}\tau_w d^2, \tag{2}$$

the flow being assumed to be incompressible. The calibration curve can thus be expressed as

$$\frac{d'}{d} = F(R_s). \tag{3}$$

In what follows it is sometimes found convenient to refer to the quantity R_s as the 'Stanton-tube Reynolds number', although if τ_w is thought of as being density times friction velocity squared, R_s has the appearance of a Reynolds number squared. However, if τ_w is thought of as being viscosity times velocity gradient, R_s does have the appearance of a Reynolds number, and for a case where the upstream velocity profile is linear, R_s is the Reynolds number based on the tube height d and the velocity at distance d from the wall.

Another result, true when the profile is linear, is that d' then represents the position of the 'effective centre' of the tube; for $(2\Delta p/\rho)^{1/2}$ can be regarded as the velocity measured by the tube, so that the right-hand side of equation (1) is the distance from the wall at which the velocity in the upstream linear profile is equal to that measured.

* Published with the permission of the Director, National Physical Laboratory.

The calibration curve (equation (3)) is assumed to apply if the Stanton tube is used to measure the skin friction in a boundary layer, so that τ_w can be found from the measured value of Δp. The validity of this procedure is discussed in Ref. 3. In particular it is shown that if the instrument is to be used to measure the skin friction in a turbulent boundary layer, it should be calibrated in turbulent flow. This is because of Bradshaw's finding[4] that the calibration function $F(R_s)$ is not the same for turbulent flow as it is for laminar flow. This difference partly arises from the fact that for values of R_s greater than about 30, the height d of the tube will be greater than half the sublayer thickness in turbulent flow (*cf.* Ref. 3). Thus in turbulent flow at high Reynolds numbers the velocity profile will not be linear over the region influenced by the tube, whereas in laminar flow the profile probably will be effectively linear. The presence of velocity fluctuations within the laminar sublayer may also contribute to the difference between the laminar and turbulent calibration results, as Bradshaw[4] has pointed out.

Fig. 2 shows some calibration results for laminar and turbulent flow. For the laminar curve a smooth join has been made between Taylor's results[2] for very low Reynolds numbers and Hool's results[5] at moderate Reynolds numbers. To draw a single curve in this way may not be justifiable because the tubes used by Taylor and Hool were probably not geometrically similar in such respects as the proportion of the total tube height d comprised by the opening (*cf.* Fig. 1). However, in turbulent flow it seems that the precise geometry of the tube may not matter, since Bradshaw's data[4], obtained with tubes whose shapes differed somewhat, all lie roughly on a smooth curve, which is reproduced in Fig. 2. Thus for turbulent flow, and possibly also for laminar, the pressure recorded by most forms of Stanton tube would probably be much the same as the pressure in the corner at the bottom of a solid step of the same height d as the tube, as shown in Fig. 3.

If such a step were placed in a uniform laminar shear flow, d' corresponding to the pressure in the corner would vary with Reynolds number in a similar way to the laminar curve in Fig. 2. It would be of interest to try to predict theoretically the calibration curve for this apparently simple case of a step in a linear velocity gradient.

In fact the problem is far from simple, since the full Navier-Stokes equations are involved. Consider a co-ordinate system as shown in Fig. 3 with its origin at the bottom of the step. X and Y are the physical lengths, and the corresponding velocities are U and V. The equations can be written in non-dimensional form by making the substitutions

$$\left.\begin{aligned} x &= \frac{X}{d}, \quad y = \frac{Y}{d} \\ \frac{\partial \psi}{\partial y} &= \frac{U\mu}{d\tau_w}, \quad \frac{\partial \psi}{\partial x} = -\frac{V\mu}{d\tau_w} \end{aligned}\right\}, \tag{4}$$

where τ_w is the friction stress at the wall for $x \to -\infty$. Then $x = 0$, $0 \leqslant y \leqslant 1$ represents the vertical face of the step, $x > 0$, $y = 1$ represents the top of the step, and $x < 0$, $y = 0$ is the wall upstream of the step. Hence the boundary conditions are

$$\left.\begin{aligned} \psi, \frac{\partial \psi}{\partial y}, \frac{\partial \psi}{\partial x} = 0 \text{ for } & x < 0, y = 0 \\ & x = 0, 0 \leqslant y \leqslant 1 \\ & x > 0, y = 1 \end{aligned}\right\}. \tag{5}$$

Also, since the upstream profile is linear,

$$\frac{\partial^2\psi}{\partial y^2} \to 1 \text{ as } x \to -\infty . \tag{6}$$

The continuity equation is automatically satisfied by ψ, and the X and Y component momentum equations become respectively

$$\frac{1}{\tau_w}\frac{\partial p}{\partial x} = \frac{\partial^3\psi}{\partial x^2\partial y} + \frac{\partial^3\psi}{\partial y^3} - R_s\left[\frac{\partial\psi}{\partial y}\frac{\partial^2\psi}{\partial y\partial x} - \frac{\partial\psi}{\partial x}\frac{\partial^2\psi}{\partial y^2}\right], \tag{7}$$

$$\frac{1}{\tau_w}\frac{\partial p}{\partial y} = -\frac{\partial^3\psi}{\partial x^3} - \frac{\partial^3\psi}{\partial y^2\partial x} - R_s\left[-\frac{\partial\psi}{\partial y}\frac{\partial^2\psi}{\partial x^2} + \frac{\partial\psi}{\partial x}\frac{\partial^2\psi}{\partial x\partial y}\right], \tag{8}$$

where p is the physical pressure. Eliminating p we obtain

$$\frac{\partial^4\psi}{\partial y^4} + 2\frac{\partial^4\psi}{\partial y^2\partial x^2} + \frac{\partial^4\psi}{\partial x^4} = R_s\left\{\frac{\partial\psi}{\partial y}\left[\frac{\partial^3\psi}{\partial x^3} + \frac{\partial^3\psi}{\partial x\partial y^2}\right] - \frac{\partial\psi}{\partial x}\left[\frac{\partial^3\psi}{\partial y^3} + \frac{\partial^3\psi}{\partial x^2\partial y}\right]\right\} . \tag{9}$$

It is clearly a formidable task to obtain solutions of (9) under the boundary conditions (5) and (6). For very low Reynolds number the problem is simplified, since the terms on the right-hand side of (9) can presumably be neglected, giving a solution for ψ which is a function of x and y only, independent of R_s. Along the wall upstream of the step equation (7) reduces to

$$\frac{1}{\tau_w}\frac{\partial p}{\partial x} = \left(\frac{\partial^3\psi}{\partial y^3}\right)_{y=0}$$

in virtue of (5). Hence, if the pressure at the bottom of the step is greater by Δp than the pressure far upstream,

$$\Delta p = \tau_w \int_{-\infty}^{0} \left(\frac{\partial^3\psi}{\partial y^3}\right)_{y=0} dx$$

and from (1) and (2)

$$\frac{d'}{d} = \left[\frac{2}{R_s}\int_{-\infty}^{0}\left(\frac{\partial^3\psi}{\partial y^3}\right)_{y=0} dx\right]^{1/2} . \tag{10}$$

In general the integral here is itself a function of R_s, but this is not so for low values of R_s, when ψ is a function only of x and y, so that d'/d is proportional to $R_s^{-1/2}$, as found by Taylor[2] experimentally. Whilst it is easy to get thus far, it is difficult to find the numerical value of the factor of proportionality, since this involves solving for ψ. Dean[6, 7, 8] has attempted the problem analytically, and Thom[9] has obtained a numerical solution, but all these methods are necessarily laborious.

When the Reynolds number is not very low the situation is still worse, since it is not even possible to determine the power of R_s to which d'/d is proportional. Trilling and Häkkinen[10] attempted to find a solution for large values of R_s, but their work is open to objections. They write

$$\left.\begin{aligned}\frac{\partial\psi}{\partial y} &= y + \bar{u}\\ \eta &= yR_s^{1/3}\end{aligned}\right\}, \tag{11}$$

assuming that derivatives of quantities with respect to η are of the same order as derivatives with respect to x. Far upstream of the step $\bar{u} \to 0$, from (6) and (11). Accordingly, in equation (9) the

right-hand side is linearised, terms involving products of $\bar{u}$ or its derivatives being neglected. Thus for large values of R_s the equation reduces to

$$\frac{\partial^3 \bar{u}}{\partial \eta^3} = \eta \frac{\partial^2 \bar{u}}{\partial x \partial \eta} .$$

Trilling and Häkkinen make the reasonable assumption that the flow separates from the wall at some distance Ld upstream of the step, as shown in Fig. 4, so that $(x = -L, \eta = 0)$ is the separation point. Then they assume that the boundary conditions (5) may be replaced by the approximate conditions

$$\left.\begin{aligned} \bar{u} &= 0 \qquad \text{for } \eta = 0, \ -\infty < x < -L \\ \bar{u} &= \frac{x}{L} + 1 \text{ for } \eta = 0, \ -L < x < 0 \end{aligned}\right\} .$$

This allows for the velocity being non-zero on the streamline which divides the main flow from the region of separation. The dividing streamline can, it is supposed, be treated as though it were flat down on the wall upstream of the step, and the flow inside the separated region is ignored. With these assumptions a solution can be found with $\bar{u}$ a function of x/L and $\eta/L^{1/3}$ only, independent of R_s. Thus $(\partial^3\psi/\partial y^3)_{y=0}$ in equation (10) becomes proportional to $L^{-2/3}R_s^{2/3}$, and d'/d to $L^{1/6}R_s^{-1/6}$. However, since the dividing streamline must in reality terminate near the top corner of the step, which is at $\eta = R_s^{1/3}$, the assumption that η can be treated as zero along the streamline would seem to be invalid. A further objection to the solution concerns the linearisation applied to the right-hand side of (9), since it can be shown that, except far upstream, the neglected non-linear terms are probably bigger than the linear terms included. Finally, Trilling and Häkkinen assume L to be constant, so that d'/d is, according to their solution, proportional to $R_s^{-1/6}$. However, in reality the separation position is quite likely to vary with Reynolds number, so that even if their solution were valid, d'/d might be proportional to some different power of R_s.

Difficulties with regard to the boundary conditions similar to those encountered in Trilling's and Häkkinen's method arise if it is attempted to stretch the co-ordinates in any other simple way, so as to obtain a solution for ψ in the stretched co-ordinates which shall be independent of R_s at large R_s. The simple possibility that the left-hand side of (9) can be neglected because of the factor R_s on the other side is of course ruled by the boundary conditions (5). Thus the mode of variation of d'/d with R_s cannot easily be found even when R_s is large. However, a crude order-of-magnitude estimation of d'/d can be made as follows:

Suppose that at $y = n$, $Y = nd$, there is a wall moving with velocity $nd\tau_w/\mu$, as in Fig. 5. Then far upstream of the step this will produce a Couette flow with a linear velocity profile, and for all values of x

$$\psi = \frac{n^2}{2}, \ \frac{\partial \psi}{\partial y} = n \text{ at } y = n . \tag{12}$$

Provided n is not too small the flow over the step will approximate closely to what it would be in an infinite uniform shear flow. This is because with an infinite shear flow the streamlines some distance away from the wall would, as indicated in Fig. 4, be effectively undisturbed by the step, continuity considerations requiring the disturbance to the streamlines to decrease more rapidly with distance than it would if the flow over the step were inviscid, with a uniform velocity upstream.

Let the fixed boundary including the step be denoted by A and the moving wall by B. Then if equation (9) is integrated between A and B with respect to y at a constant x there results in virtue of equation (7) and the boundary conditions (5) and (12)

$$\frac{1}{\tau_w}\frac{d}{dx}(p_A - p_B) = \frac{d^4}{dx^4}\int_A^B \psi\, dy - R_s \frac{d}{dx}\int_A^B \frac{\partial\psi}{\partial y}\frac{\partial^2\psi}{\partial x^2}\, dy\,.$$

Hence for $x \leqslant 0$,

$$\frac{1}{\tau_w}(p_A - p_B) = \frac{d^3}{dx^3}\int_A^B \psi\, dy - R_s\int_A^B \frac{\partial\psi}{\partial y}\frac{\partial^2\psi}{\partial x^2}\, dy\,, \tag{13}$$

since for $x \to -\infty$, $p_A = p_B = p_0$ and the terms on the right-hand side are zero. At $x = 0$, $p_A = p_0 + \Delta p$, but p_B will only differ slightly from p_0 if n is sufficiently large. Hence from (1) and (2)

$$\frac{d'}{d} \doteq \left\{\frac{2}{R_s}\frac{d^3}{dx^3}\int_A^B \psi\, dy - 2\int_A^B \frac{\partial\psi}{\partial y}\frac{\partial^2\psi}{\partial x^2}\, dy\right\}_{x=0}^{1/2}. \tag{14}$$

Suppose that separation occurs at $x = -L$, as indicated in Fig. 5. For this value of x also p_B will differ little from p_0, so from equations (7) and (13)

$$\int_{x=-L}^{0}\left(\frac{\partial^3\psi}{\partial y^3}\right)_A dx \doteq \left\{\frac{d^3}{dx^3}\int_A^B \psi\, dy\right\}_{x=0} - \left\{\frac{d^3}{dx^3}\int_A^B \psi\, dy\right\}_{x=-L} -$$
$$- \left\{R_s\int_A^B \frac{\partial\psi}{\partial y}\frac{\partial^2\psi}{\partial x^2}\, dy\right\}_{x=0} + \left\{R_s\int_A^B \frac{\partial\psi}{\partial y}\frac{\partial^2\psi}{\partial x^2}\, dy\right\}_{x=-L}. \tag{15}$$

This equation is the double integral with respect to x and y of the full equation (9) over the shaded area in Fig. 5. The shape of the distribution of ψ in this region may roughly be guessed because of the restrictions imposed on ψ by the boundary conditions (5) and (12) and by the assumption of a separated flow with an approximately straight dividing streamline where $\psi = 0$, as in Fig. 5. Thus ψ can be represented by a polynomial distribution in y, with coefficients which are polynomials in x, between the dividing streamline and the wall B, whilst between the dividing streamline and the wall A, ψ is represented by a second polynomial distribution joining on to the first. If ψ is to be guessed in this way, however, n must not be made too large. Nor of course must it be made too small, because then the pressure distribution along the wall A would differ appreciably from what it would be in an infinite flow field. The optimum value for n corresponds in the infinite flow-field case to the distance from the wall A of the nearest streamline to be virtually undisturbed by the presence of the step. A larger assumed value of n would include too much undisturbed flow, and the boundary conditions (12) would not have their proper influence on the shape of the assumed distribution for ψ. The situation is analogous to Pohlhausen's well-known method[11] for boundary layers, where boundary conditions which are strictly valid only at infinity are transferred to a distance δ from the wall, δ being the effective total thickness of the boundary layer.

In Pohlhausen's method δ is not known beforehand, but has to be found from the solution. Similarly in the present instance the distance to the nearest undisturbed streamline is not known, and neither is the separation position. Hence L and n appear as parameters in the assumed distribution for ψ, and the integral equation (15) gives a relation between them. Two different families of assumed distributions for ψ (polynomials as discussed above) were considered. With

either family, ψ is a function of y and x/L for a given n. Hence, when the Reynolds number R_s is very large, (15) gives a relation of the form

$$L = R_s^{1/3} F(n) . \tag{16}$$

Then (14) results in

$$\frac{d'}{d} = R_s^{-1/3} G(n) . \tag{17}$$

A similar procedure may be adopted when the Reynolds number is not large, but unless the assumed distribution for ψ is close to the real distribution, the answers are likely to suffer from bigger errors than those obtained for high Reynolds numbers. This is because the first two terms on the right-hand side of (15) involve a higher-order derivative than the other two terms.

For high Reynolds numbers, the two different assumed families of distributions for ψ gave much the same results for $G(n)$ in equation (17), and moreover G was found not to vary much with n, as can be seen from the following Table:

n		2	4	6	8	10
Family 1 results	F	0·99	1·62	2·31	2·99	3·71
	G	2·82	2·63	2·72	2·87	2·99
Family 2 results	F	1·32	2·35	3·38	4·39	5·40
	G	3·12	2·92	3·00	3·20	3·47

Thus a wide variety of assumed distributions for ψ all gave results for d'/d close to $3R_s^{-1/3}$, and this suggests that if ψ could be guessed correctly much the same answer would be obained; in other words, that $3R_s^{-1/3}$ is fairly close to the correct form for d'/d. Hool's result[5] $d'/d = 1{\cdot}8R_s^{-1/5}$ is in fact of the same order as $3R_s^{-1/3}$ for $10 < R_s < 1000$, as can be seen from Fig. 2, and since the above crude analysis can only be expected to give an order-of-magnitude estimation, the agreement is satisfactory. As it happens, the turbulent calibration results shown in Fig. 2 appear to be approaching the curve $3R_s^{-1/3}$ at high Reynolds numbers, though the theory can hardly be valid for such conditions.

Equation (16) and the results of the Table also show that if n were large L would probably be very large at large Reynolds numbers. Trilling and Häkkinen[10] found experimentally that L was typically between 4 and 20. This suggests that at Reynolds numbers R_s of 1000, say, n ought not to be greater than about 4. At low Reynolds numbers it would seem from the work of Dean[6, 7, 8] and Thom[9] that n, the distance from the wall to the nearest effectively undisturbed streamline, is in the region of 6 to 10. Hence it may well be that if a Stanton tube in a boundary layer is to read approximately the same as in an infinite uniform shear flow with the same skin friction, the velocity profile need only be linear for about 4 tube heights at Reynolds numbers of about 1000, whereas the linear part of the profile would need to extend further at low Reynolds numbers.

An experiment to test these conjectures is in hand.

Acknowledgements.—Discussions with Mr. P. Bradshaw on the subject of turbulent calibration results, and with Dr. R. C. Lock concerning Trilling's and Häkkinen's solution, were most helpful.

LIST OF SYMBOLS

d		Height of Stanton tube above surrounding surface
d'		Defined by equation (1): 'effective centre' position for linear-profile case
L		Distance of separation position in tube heights upstream of Stanton tube
n		Distance of moving wall in tube heights from fixed wall in model of Fig. 5: for infinite flow field n corresponds to position of nearest effectively undisturbed streamline
p		Pressure
Δp		Excess of pressure recorded by Stanton tube over static pressure
R_s		Defined by equation (2): can be regarded as Stanton-tube Reynolds number
U		Physical velocity parallel to wall
$\bar{u}$		Defined by equation (11): proportional to difference between velocity at a general point and velocity at same y upstream
V		Physical velocity normal to wall
X		Physical length parallel to wall
x	$=$	X/d
Y		Physical length normal to wall
y	$=$	Y/d
η	$=$	$yR_s^{1/3}$
μ		Viscosity
ρ		Density
τ_w		Skin friction for undisturbed profile upstream of Stanton tube
ψ		Non-dimensional stream function defined by equations (4).

REFERENCES

No.	*Author*	*Title, etc.*
1	T. E. Stanton, D. Marshall and L. Bryant	On the conditions at the boundary of a fluid in turbulent motion. *Proc. Roy. Soc.* A. 97. 422. 1920.
2	G. I. Taylor	Measurements with a half-pitot tube. *Proc. Roy. Soc.* A. 166. 476. 1938.
3	G. E. Gadd, W. F. Cope and J. L. Attridge	Heat transfer and skin friction measurements at a Mach number of 2·44 for a turbulent boundary layer on a flat surface and in regions of separated flow. R. & M. 3148. October, 1958.
4	P. Bradshaw and N. Gregory	Report on the determination of local turbulent skin friction from observations in the viscous sublayer. (In preparation.)
5	J. N. Hool	Measurements of skin friction using surface tubes. *Airc. Eng.* 28. 52. 1956.
6	W. R. Dean	Note on the slow motion of fluid. *Phil. Mag.* 15. 929. 1933.
7	W. R. Dean	Note on the slow motion of fluid. *Proc. Camb. Phil. Soc.* 32. 598. 1936.
8	W. R. Dean	Slow motion of viscous liquid near a half-pitot tube. *Proc. Camb. Phil. Soc.* 48. 149. 1952.
9	A. Thom	The flow at the mouth of a Stanton pitot. R. & M. 2984. October, 1952.
10	L. Trilling and R. J. Häkkinen	The Calibration of the Stanton Tube as a Skin-Friction Meter. *50 Jahre Grenzschichtforschung.* 201. 1955 (Published by Friedr. Vieweg & Sohn, Braunschweig).
11	K. Pohlhausen	Zur näherungsweisen Integration der Differentialgleichung der laminaren Grenzschicht. *Z.A.M.M.* 1. 252. 1921.

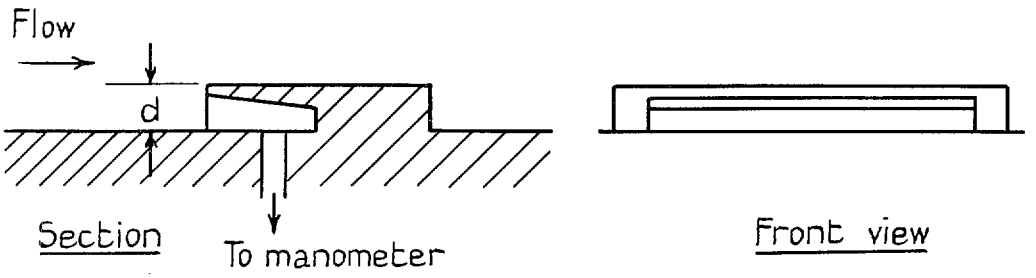

FIG. 1. A typical Stanton tube.

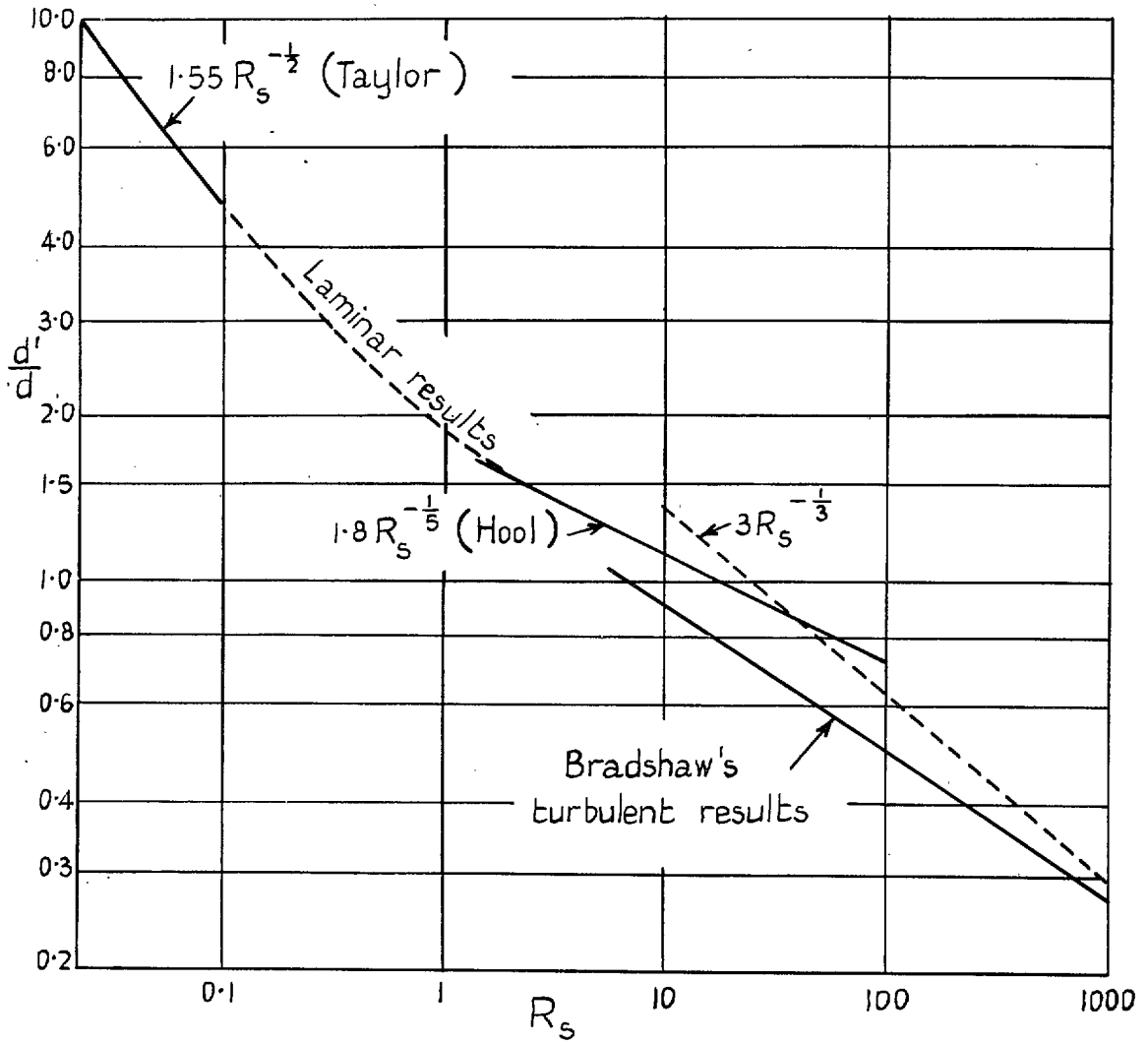

FIG. 2. Stanton-tube calibration results.

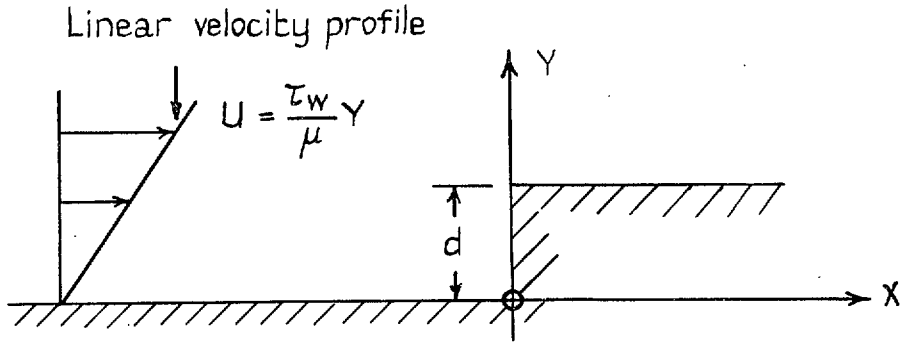

FIG. 3. Solid step equivalent to Stanton tube.

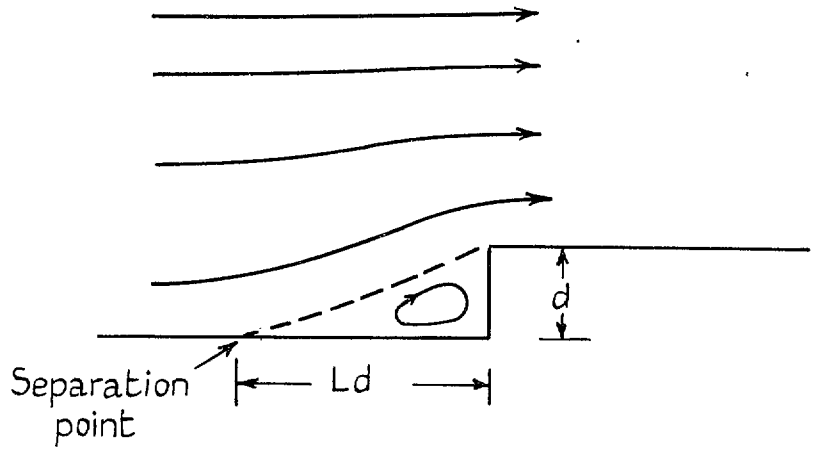

FIG. 4. Streamline pattern showing separation.

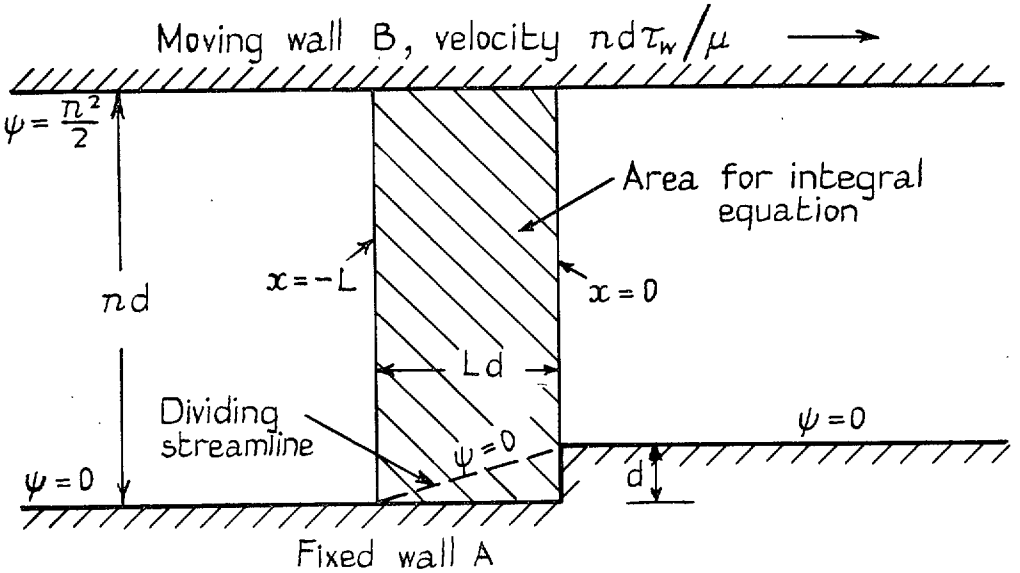

FIG. 5. Model considered in analysis.

(78643) Wt. 54/8210 K.5 2/60 Hw.

Publications of the Aeronautical Research Council

ANNUAL TECHNICAL REPORTS OF THE AERONAUTICAL RESEARCH COUNCIL (BOUND VOLUMES)

1941 Aero and Hydrodynamics, Aerofoils, Airscrews, Engines, Flutter, Stability and Control, Structures. 63*s.* (post 2*s.* 3*d.*)

1942 Vol. I. Aero and Hydrodynamics, Aerofoils, Airscrews, Engines. 75*s.* (post 2*s.* 3*d.*)
Vol. II. Noise, Parachutes, Stability and Control, Structures, Vibration, Wind Tunnels. 47*s.* 6*d.* (post 1*s.* 9*d.*)

1943 Vol. I. Aerodynamics, Aerofoils, Airscrews. 80*s.* (post 2*s.*)
Vol. II. Engines, Flutter, Materials, Parachutes, Performance, Stability and Control, Structures. 90*s.* (post 2*s.* 3*d.*)

1944 Vol. I. Aero and Hydrodynamics, Aerofoils, Aircraft, Airscrews, Controls. 84*s.* (post 2*s.* 6*d.*)
Vol. II. Flutter and Vibration, Materials, Miscellaneous, Navigation, Parachutes, Performance, Plates and Panels, Stability, Structures, Test Equipment, Wind Tunnels. 84*s.* (post 2*s.* 6*d.*)

1945 Vol. I. Aero and Hydrodynamics, Aerofoils. 130*s.* (post 2*s.* 9*d.*)
Vol. II. Aircraft, Airscrews, Controls. 130*s.* (post 2*s.* 9*d.*)
Vol. III. Flutter and Vibration, Instruments, Miscellaneous, Parachutes, Plates and Panels, Propulsion. 130*s.* (post 2*s.* 6*d.*)
Vol. IV. Stability, Structures, Wind Tunnels, Wind Tunnel Technique. 130*s.* (post 2*s.* 6*d.*)

Special Volumes

Vol. I. Aero and Hydrodynamics, Aerofoils, Controls, Flutter, Kites, Parachutes, Performance, Propulsion, Stability. 126*s.* (post 2*s.* 6*d.*)
Vol. II. Aero and Hydrodynamics, Aerofoils, Airscrews, Controls, Flutter, Materials, Miscellaneous, Parachutes, Propulsion, Stability, Structures. 147*s.* (post 2*s.* 6*d.*)
Vol. III. Aero and Hydrodynamics, Aerofoils, Airscrews, Controls, Flutter, Kites, Miscellaneous, Parachutes, Propulsion, Seaplanes, Stability, Structures, Test Equipment. 189*s.* (post 3*s.* 3*d.*)

Reviews of the Aeronautical Research Council

1939–48 3*s.* (post 5*d.*) 1949–54 5*s.* (post 6*d.*)

Index to all Reports and Memoranda published in the Annual Technical Reports

1909–1947 R. & M. 2600 6*s.* (post 4*d.*)

Author Index to the Reports and Memoranda and Current Papers of the Aeronautical Research Council

February, 1954–February, 1958 R. & M. No. 2570 (Revised) (Addendum) 7*s.* 6*d.* (post 4*d.*)

Indexes to the Technical Reports of the Aeronautical Research Council

July 1, 1946–December 31, 1946 R. & M. No. 2150 1*s.* 3*d.* (post 2*d.*)

Published Reports and Memoranda of the Aeronautical Research Council

Between Nos. 2251–2349	R. & M. No. 2350 1*s.* 9*d.* (post 2*d.*)
Between Nos. 2351–2449	R. & M. No. 2450 2*s.* (post 2*d.*)
Between Nos. 2451–2549	R. & M. No. 2550 2*s.* 6*d.* (post 2*d.*)
Between Nos. 2551–2649	R. & M. No. 2650 2*s.* 6*d.* (post 2*d.*)
Between Nos. 2651–2749	R. & M. No. 2750 2*s.* 6*d.* (post 2*d.*)
Between Nos. 2751–2849	R. & M. No. 2850 2*s.* 6*d.* (post 2*d.*)
Between Nos. 2851–2949	R. & M. No. 2950 3*s.* (post 2*d.*)

HER MAJESTY'S STATIONERY OFFICE

from the addresses overleaf

Printed and published by
HER MAJESTY'S STATIONERY OFFICE

To be purchased from
York House, Kingsway, London W.C.2
423 Oxford Street, London W.1
13A Castle Street, Edinburgh 2
109 St. Mary Street, Cardiff
39 King Street, Manchester 2
Tower Lane, Bristol 1
2 Edmund Street, Birmingham 3
80 Chichester Street, Belfast 1
or through any bookseller

Printed in England

S.O. Code No. 23-3147